Available online at www.CivileJournal.org

Civil Engineering Journal

(E-ISSN: 2476-3055; ISSN: 2676-6957)

Vol. 11, No. 05, May, 2025

Experimental and Numerical Analysis of the Behavior of Steel Scaffolding

Florim Grajçevci [1], Armend Mujaj [1*], Driton Kryeziu [2], Elfrida Shehu [3], Zijadin Guri [1]

[1] *Faculty of Civil Engineering, University of Pristina, Pristina, Kosovo.*

[2] *Civil Engineering and Infrastructure Department, University for Business and Technology UBT, Pristina, Kosovo.*

[3] *Polytechnic University of Tirana, Tirana, Albania.*

Received 25 January 2025; Revised 16 April 2025; Accepted 21 April 2025; Published 01 May 2025

Abstract

In recent days, due to the reduction in the labor force, investment in construction equipment has become increasingly common to compensate for the shortage of workers. Among other equipment, scaffolding—both external and internal—plays a crucial role during the construction phase of buildings. Scaffolds are among the components that require special attention, as they are directly linked to the health and safety of workers. For this reason, they have received significant attention in recent years following frequent collapse incidents. Any defect in the construction or use of scaffolding can pose serious, even fatal, risks to workers. Therefore, the safety and stability of scaffolds are essential for preventing accidents and protecting the lives of those working on construction sites, especially those working at great heights. This study analyzes scaffolding with a height of 200 cm, treating it in a spatial manner to calculate the maximum load-bearing capacity, lateral and vertical displacements, as well as to assess the stress and deformation states in the vertical elements (columns). This process was carried out by applying the rules of Eurocode EN 1993-1-1, along with experimental analysis and calculations using the SEIMOSOFT application software.

Keywords: Steel Scaffold; Circular Hollow Section; European Standards; Strain Gauges.

1. Introduction

Scaffolding is classified as a temporary structure, primarily used in construction to support various types of loads, including the workforce, work equipment, and construction materials. Based on their use, scaffolds can be external, mainly used to support the façade during the construction phase or for the rehabilitation of various elements, and internal scaffolds, which are used to support the mass of fresh concrete during the casting of horizontal, inclined, or vertical structural elements, where they may also function as formwork. The static analysis of scaffolds is usually performed in the elastic stage, where a linear relationship between stress and strain is assumed. The calculation process is similar to that of load-bearing structural elements: first, the load analysis is performed, followed by the determination of static effects. Then, the stability of the structure is checked based on the rules of design codes [1-4]. In recent years, with the increase in economic development, the construction of buildings with complex architectural forms has also increased, which has brought about a continuous need for technological advancement and improvement of formwork types, as they play a key role in the construction process. Formwork directly affects the time, quality, and cost of construction [5, 6].

The positioning of scaffolds typically consists of elements with hollow circular cross-sections, as these are easier to handle. Scaffolds can be made from various materials, such as steel, certain alloys like aluminum, but also from wood in special cases. From a configuration standpoint, scaffolds can be interconnected systems, such as pairs, or

* Corresponding author: armend.mujaj@uni-pr.edu

http://dx.doi.org/10.28991/CEJ-2025-011-05-014

standalone elements, depending on the manufacturer and the specific requirements related to their load-bearing capacity [7-9]. To ensure the proper stability of scaffolds and to withstand the anticipated loads, it is essential that the connections between elements are effective. For this reason, a study on this phenomenon has been conducted as part of this research [10-12].

In the case of connected or paired scaffolds, the position of bracing plays a significant role in their load-bearing capacity. A study on the effect of bracing in relation to load-bearing capacity was conducted in Do Lee et al. [13], where the influence of bracing position on the stability and performance of scaffolds was analyzed. Based on the method of ground support and the placement of bracing, the selection of the static scheme and the buckling length play an important role in scaffold calculations. This phenomenon, which examines the effect of buckling length and compares load-bearing capacity in relation to static schemes, is addressed in Takahashi et al. [14]. The positioning of scaffolds can be either static or mobile, depending on usage requirements. A study on the stability of mobile scaffolds was conducted by the authors in Kim et al. [15].

In cases where scaffolds are connected vertically (multi-level scaffolding), the stiffness of the joint connections has a direct impact on their load-bearing capacity. A study in this area was carried out by the authors in their work, examining how the stiffness of these connections affects the performance and stability of the scaffolding [16, 17]. When calculating steel elements such as scaffold columns, in addition to the many factors that influence load-bearing capacity, imperfections also play an important role. This phenomenon has been analyzed within the referenced studies [18, 19].

1.1. Research Significance

The aim of this study was to present the behavior of scaffolds with a height of H = 200 cm, made of steel with hollow circular cross-sections, under the influence of axial compressive force. These scaffolds were tested as spatial systems, analyzing and comparing the experimentally obtained values with theoretical ones according to EN 1993-1-1 and using the SEISMOSOFT application software. Furthermore, the output results were interpreted, including maximum force, lateral displacement at the midpoint of the column span, axial displacement, as well as the values of deformations and stresses in the steel material.

2. Experimental Program

As part of this study, testing was conducted on scaffolds designed to support fresh concrete during the casting phase of horizontal elements, classifying them as internal scaffolds. The scaffold structure consists of two frames connected at three points with horizontal elements. To ensure spatial stability, the frames are linked with bracing elements forming an 'X' shape, as illustrated in Figure 1. All scaffold components are made of metal profiles with hollow circular cross-sections. The vertical elements (columns) have dimensions of D/t = 48.3 / 3.2 mm along their entire length. To enable element continuity, the profile expands at the connection points, reaching dimensions of D/t = 57.2 / 2.9 mm. The horizontal elements, welded at three levels to the columns, have dimensions of D/t = 48.3 / 2.7 mm. Meanwhile, the bracing elements, forming an 'X'-shaped structure, have a diameter of Φ18 mm.

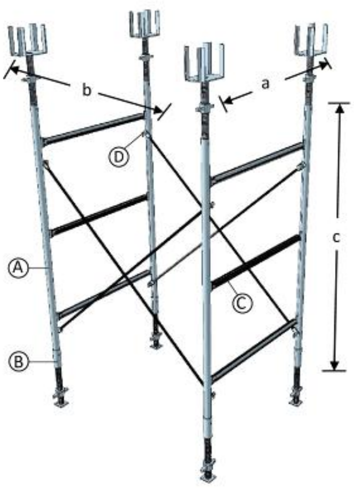

POS	D/t (mm)	L (mm)	mm
A	Ø48.3x3.2	2000	a=1150
B	Ø57.2x2.9	165	b=1500
C	Ø 48.3x2.7	1102	c=2150
D	Ø 18		

Figure 1. Representation of the scaffold dimensions and shape

In the block diagram presented in Figure 2, the calculation steps for steel elements subjected to axial compressive forces are illustrated. This process includes load calculation, cross-section classification, and verification of the stability condition, taking into account whether or not the phenomenon of buckling occurs [20].

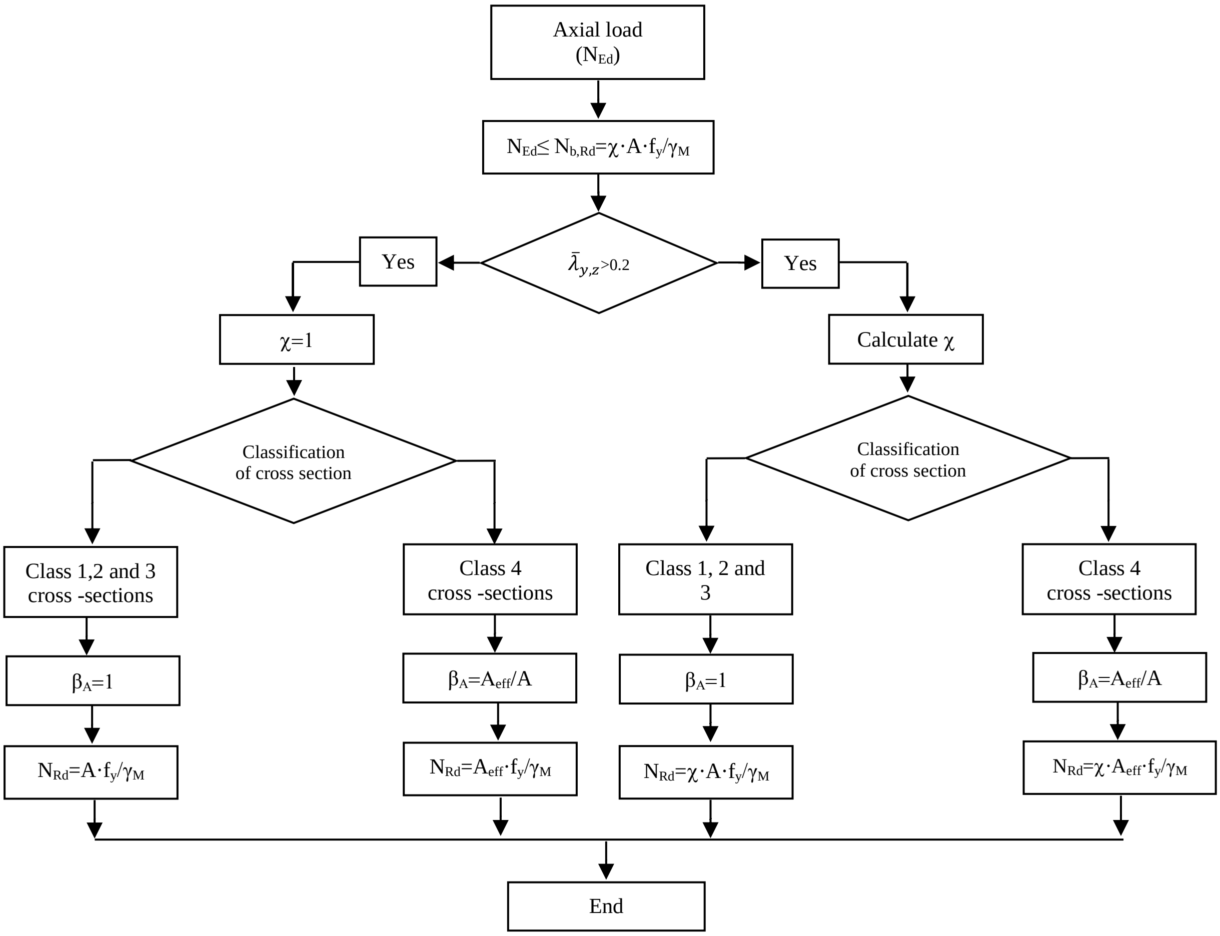

Figure 2. Flow chart for column design

The testing of the mechanical properties of the materials was carried out in accordance with ISO 6892-1:2019 [21] and EN 10002-1:2001 [22] standards. The specimens were prepared using CNC (Computer Numerical Control) equipment to ensure precise dimensions and geometry. As illustrated in Figures 3 and 4, three specimens were taken from a scaffold column, including one from the welded area, to assess the impact of the welding process on the mechanical properties of the material.

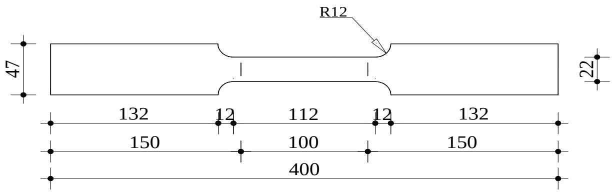

Figure 3. Test units taken from the sample columns (unit: mm)

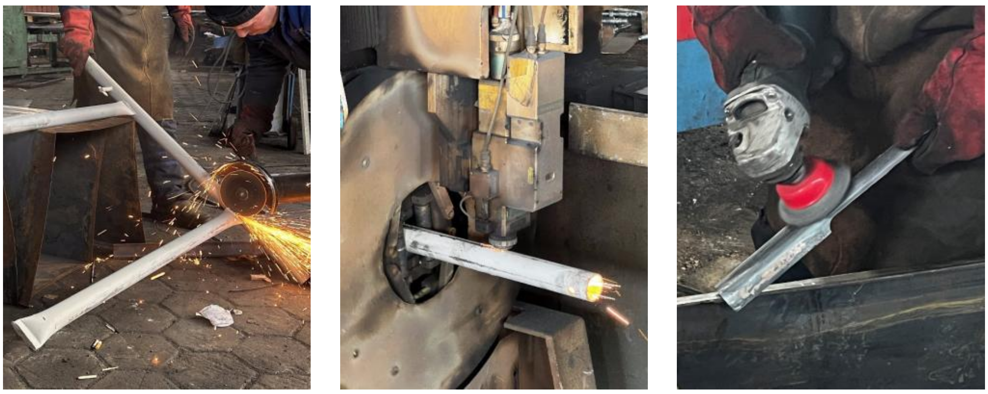

Figure 4. Cutting and preparation of the tests' samples

In Figure 4**,** the process of preparing and cutting the test tube for mechanical examination is illustrated. The first image shows the initial steel tube before cutting, while the second image captures the cutting process using a specialized machine. The final image presents the tube after being cut into a specific shape, ready for further processing and testing. In Figure 5, the examination of the mechanical properties of the material is demonstrated through three stages. Image (a) shows the extracted test specimens before undergoing any testing. Image (b) depicts one of the specimens during the mechanical testing process, where it is subjected to tensile force. Finally, image (c) presents the specimens after the final cutting, showing their shape post-testing. These steps ensure accurate evaluation of the material's mechanical behavior under different conditions.

Figure 5. Examination of the mechanical material properties

The testing of material properties was conducted at the accredited laboratory 'Proing' in Prishtina, which provides testing services in accordance with international standards. The obtained results are presented in Table 1 and include information on the mechanical properties of the tested materials. Table 1 presents the mechanical properties of the examined materials based on tensile testing of three test specimens. The table includes key parameters such as the yield force (F_m), cross-sectional area (A), yield strength (R_p) and ultimate tensile force (R_m).The results indicate slight variations in the mechanical properties among the tested specimens.

Table 1. Examination results of materials properties

Test tube	F_m(kN)	A(mm^2)	R_p(N/mm^2)	R_m(N/mm^2)
E_1*	34.89	72.1	448.5	484.1
E_2	29.62	64.0	417.9	462.7
E_3	24.76	55.0	405.4	450.2

The young modulus value is used based on the literature of Es=200,000N/mm^2

Notice *- unit taken in area of the welded unit

The testing was conducted by placing an IPE 220 metal profile in the shape of an 'H' at the top of the scaffolds. At the upper ends of the columns, supporting elements were installed to hold the 'H' metal profile, while at the lower ends, metal plate supports were placed to ensure the stability of the scaffold. This profile was used to distribute the load from the piston, transmitting it evenly to the heads of the vertical elements—the columns. Proper load distribution is essential for simulating real working conditions during the concreting process and accurately evaluating the behavior of the scaffolds under different loads, thereby contributing to increased safety and stability during construction phases. To measure scaffold displacements during testing, electronic devices called displacement sensors (LVDTs – Linear Variable Differential Transformers) were used:

- LVDT1 and LVDT3, measuring the lateral displacement in the X-X direction;
- LVDT2, measuring the displacement in the Y-Y direction;
- LVDT4, measuring the axial displacement of the scaffold members (columns).

Figure 6. Experimental Setup for Scaffold Load Testing

These measurements are crucial to obtaining accurate and reliable data on the behavior of the scaffold under loading, enabling a comparison between experimental and theoretical results while assessing the safety and stability of the structure during construction. To monitor strain and stresses in the columns, strain gauges were installed along its perimeter at a 120° angle relative to the applied force, as can be seen in Figure 7. These devices record strain at these points, providing critical data for analyzing the structural response of the column under loading.

Figure 7. Placement of Displacement Sensors and Strain Gauges during Scaffold Testing

During the testing of the scaffolds, the load was applied following the quasi-static loading protocol, aiming to replicate real-world loading conditions encountered in scaffolds during the concreting phases. This method ensures that the load is applied in a controlled manner, closely resembling the actual conditions experienced during the construction process [23]. Additionally, the reliability of the results is highly influenced by the method of load application. Therefore, it is essential to adhere to the established protocols outlined in structural testing standards to ensure that the load is applied accurately and in a controlled manner. This strict adherence enhances the precision and reliability of the test results, ultimately improving the quality and validity of the study. To ensure that the obtained results are acceptable, a calibration of the hydraulic piston was performed before starting the scaffold tests.

This calibration is a crucial step to guarantee that force measurements during testing are accurate and reliable. To further enhance the reliability of the results, the equipment used for measuring deformations, displacements, and forces is manufactured by the German company "HBK". The data collected during the tests were transformed into electronic form using the HBM Quantum X data logger and then transferred to a computer for further analysis. These devices are renowned for their accuracy and reliability, ensuring that the test data is precise and acceptable. In Figure 8, the deformation pattern of the scaffold is presented as a result of the vertical load application. This illustration demonstrates how the scaffold structure changes shape under vertical loading, including possible deformations and displacements in different sections. Analyzing these deformations is essential for understanding how the scaffold reacts to applied loads and for assessing its stability during the concreting phase or other construction loads that may be applied.

Figure 8. Scaffold deformation pre- and post-load application

The following section presents diagrams illustrating the test results, including the relationship between force and the measured displacements and deformations. These diagrams provide a detailed overview of the correlation between the applied load and scaffold behavior, showing how displacements and deformations vary depending on the applied force (Figures 9 to 13) [24-26].

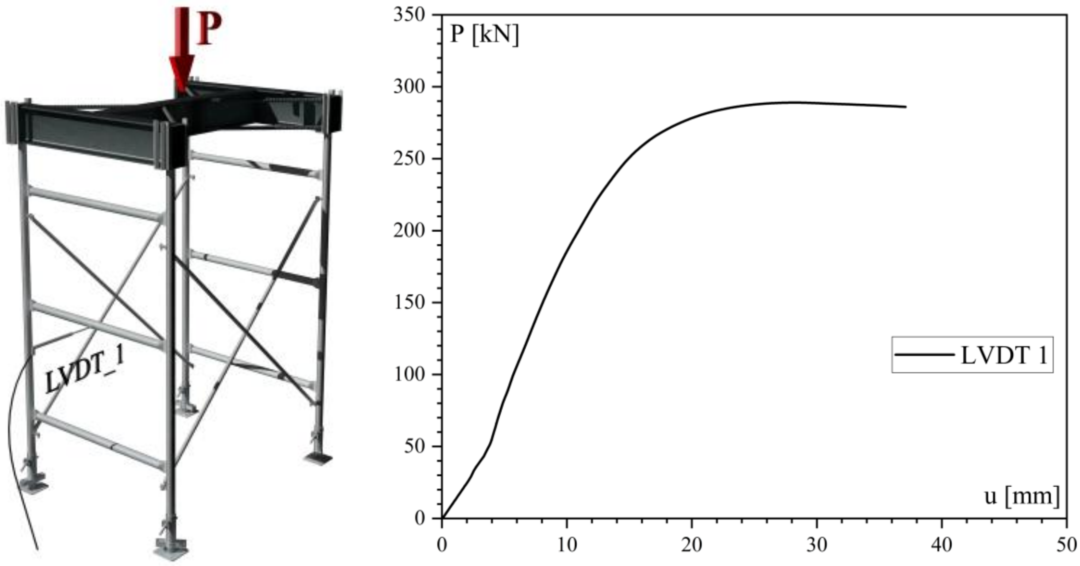

Figure 9. Force-Displacement Diagram_LVDT 1

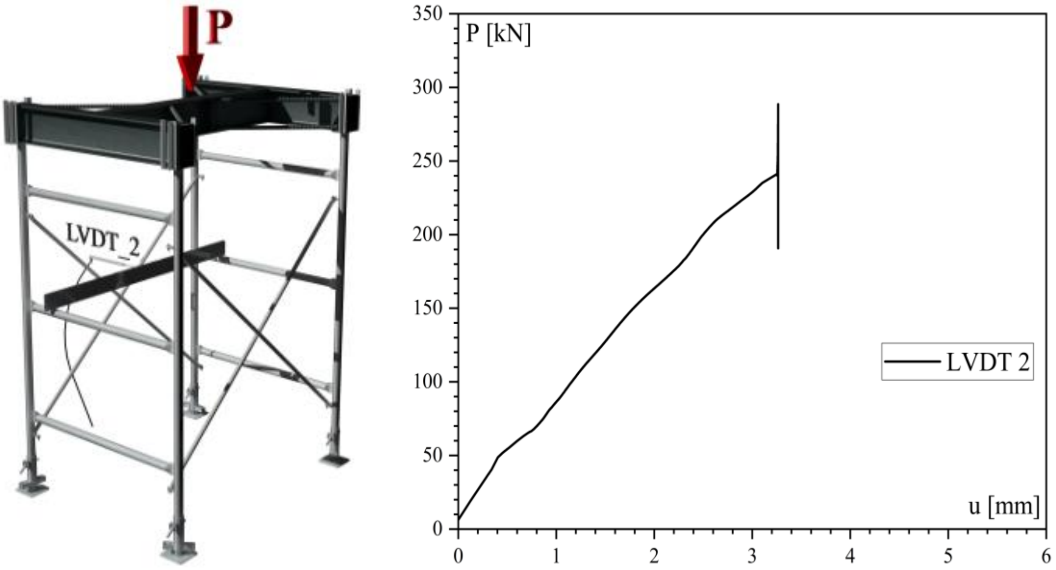

Figure 10. Force-Displacement Diagram_LVDT 2

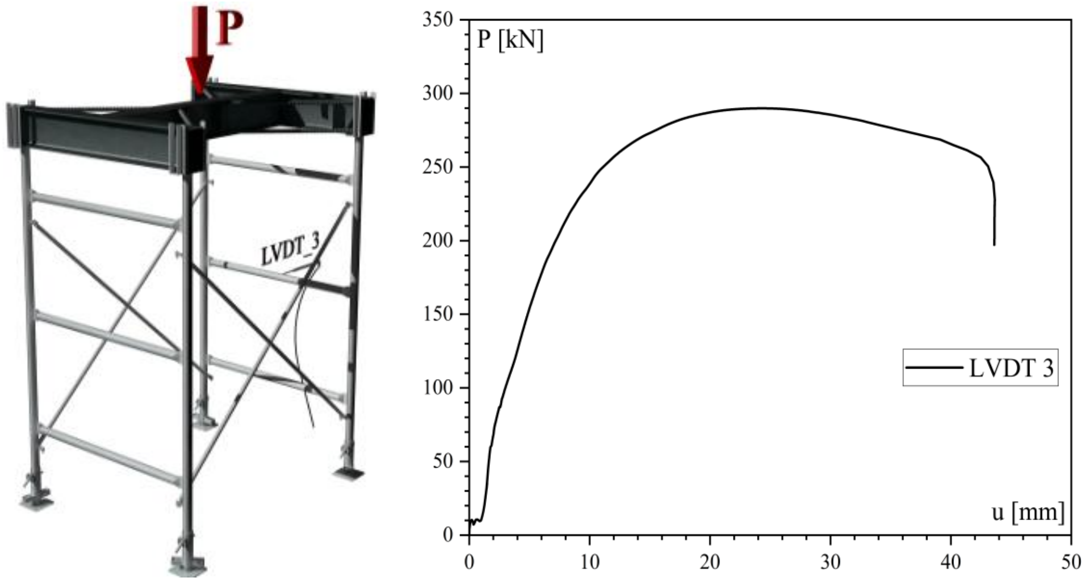

Figure 11. Force-Displacement Diagram_LVDT 3

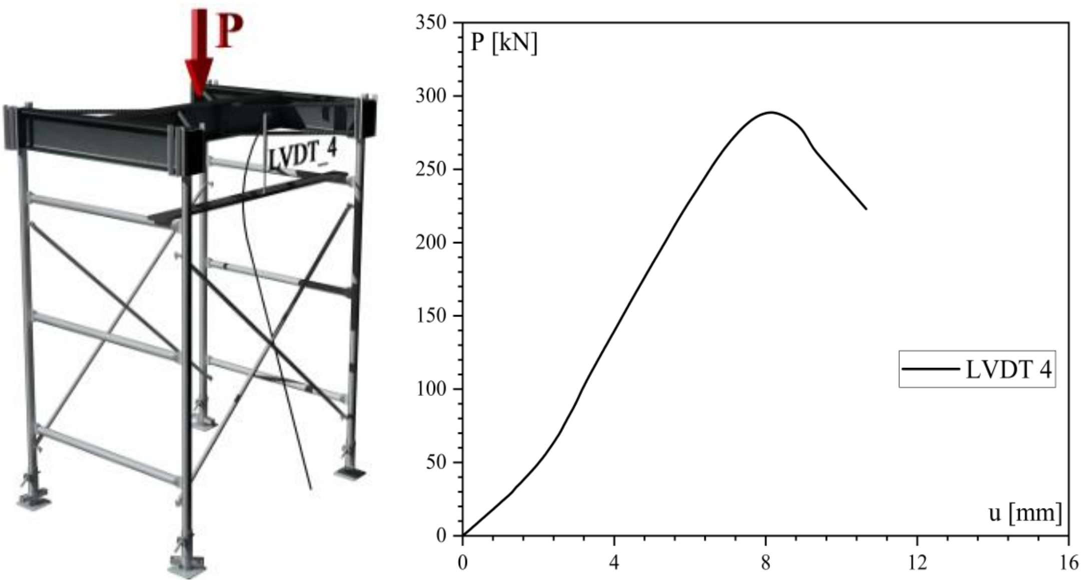

Figure 12. Force-Displacement Diagram_LVDT 4

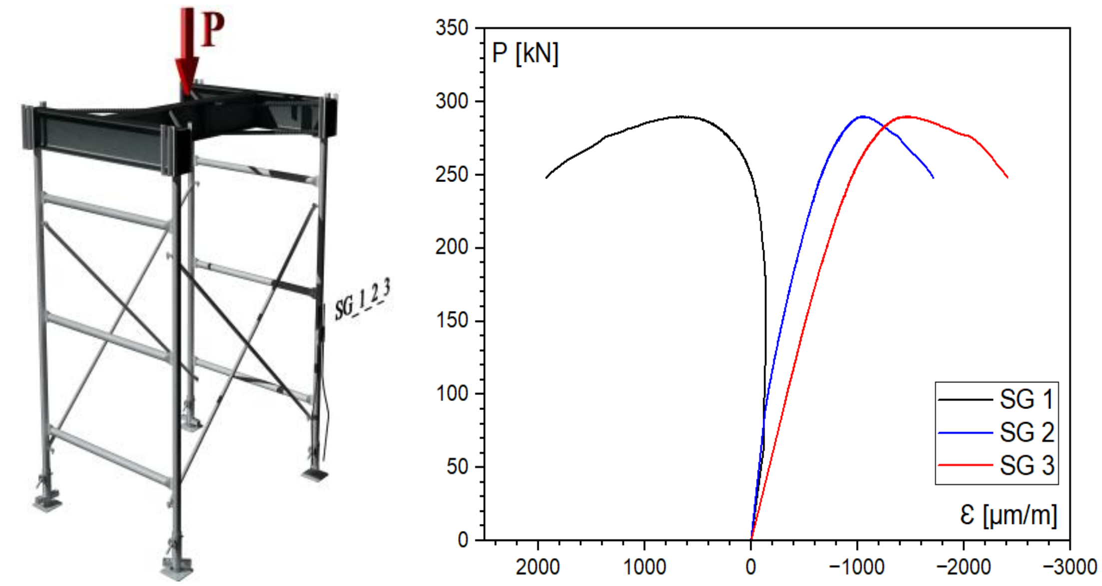

Figure 13. Force-Deformation Diagram_SG1, SG2, SG3

Based on Hooke's Law, which describes the relationship between stress and strain, the Table 2 presents the values of strain and stress at the measured positions using Strain Gauges (SG). The calculation of stresses and strains was performed using two force values, P = 200 kN and P = 292.40 kN. The results obtained from SG measurements show that under the first applied load, the entire cross-section of the scaffold column is under compression, whereas under the second load, part of the cross-section exhibits tensile stresses. This is also reflected in the deformation pattern of the scaffold, as shown in the upper sections of the study. To obtain more accurate results regarding the column's performance under load, the SGs were placed at different positions, forming an angle of 120° between them.

Table 2. Deformations and Stresses at the Measured Points

Force N (kN)	ε_1 (μm/mm)	ε_2 (μm/mm)	ε_3 (μm/mm)	σ_1 (N/mm^2)	σ_2 (N/mm^2)	σ_3 (N/mm^2)
200.00	-115.66	-452.45	-701.39	-24.15	-95.01	-147.30
292.40	647.65	-1054.50	-1467.20	129.51	-221.34	-308.11

$\sigma = \varepsilon \cdot Es$; $Es = 200000$ N/mm^2

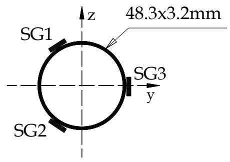

3. Theoretical Approach

For a steel element subjected to axial compressive force, where the phenomenon of buckling occurs as a result of this force, the stability condition that must be satisfied is given in the Equation 1 [3, 27].

$$\frac{N_{Ed}}{N_{b,Rd}} \leq 1.0 \tag{1}$$

where N_{Ed} is the design value of the compressive axial force, and $N_{b,Rd}$ is the design buckling resistance in compression. The design buckling resistance in compression $N_{b,Rd}$ should be taken as:

$$N_{b,Rd} = \chi \cdot \frac{N_{R,k}}{\gamma_{M1}} \tag{2}$$

where χ is the buckling reduction factor which should be determined as a function of the relative slenderness $\bar{\lambda}$ of the compression member, for the relevant buckling mode.

$$\chi = \frac{N_{b,Rd}}{N_{pl,Rd}} \tag{3}$$

The relative slenderness $\bar{\lambda}$ should be taken from Formula:

$$\bar{\lambda} = \sqrt{\frac{N_{Rk}}{N_{cr}}} \tag{4}$$

where N_{Rk} is the characteristic value of the resistance to compression, and N_{cr} is the elastic critical force for the relevant buckling mode based on the gross cross-sectional properties. The reduction factor of the non-dimensional slenderness analytically is as follows:

$$\chi = \frac{1+\alpha(\bar{\lambda}-0.2)+\bar{\lambda}^2}{2\bar{\lambda}^2} - \frac{1}{2\bar{\lambda}^2}\sqrt{\left[1+\alpha(\bar{\lambda}-0.2)+\bar{\lambda}^2\right]^2 - 4\bar{\lambda}^2} \tag{5}$$

The imperfection factor α corresponding to the appropriate buckling curve should obtained from Table 3.

Table 3. Imperfection factor for buckling curves

Buckling Curve	a_0	a	b	c	d
Imperfection factor (α)	0.13	0.21	0.34	0.49	0.76

The Equation 5 may reduce also in the straightforward way as follows:

$$\chi = \frac{1}{\Phi + \sqrt{\Phi^2 - \bar{\lambda}^2}}, \quad \text{where: } \Phi = 0.5\left[1 + \alpha(\bar{\lambda} - 0.2) + \bar{\lambda}^2\right] \tag{6}$$

where the member which are subjected to combined bending and axial compression should satisfy:

$$\frac{N_{Ed}}{\frac{\chi \cdot N_{Rk}}{\gamma_{M1}}} \leq 1 \tag{7}$$

For one of the scaffold columns, Table 4 presents the relationship between the load-bearing capacity obtained from experimental measurements, Eurocode regulations, and calculations performed using the SEISMOSOFT software.

Table 4. Examinations result of bearing capacity of the units – columns

ID	D(mm)	t(mm)	L(mm)	f_y(N/mm^2)	$N_{Exp.}$(kN)	N_{EC3}(kN)	N_{SS}(kN)	$N_{Exp.}/N_{EC3}$	$N_{Exp.}/N_{SS}$
MFRCH_2	48.30	3.20	1900	275	73.10	53.61	73.26	1.36	0.99

Additionally, Table 5 shows the ratio between the cross-sectional load-bearing capacity and the overall load-bearing capacity of the column.

Table 5. Value and ratio of the axial forces experimental force and the theoretical values of the force given by different computation methods

Method	N(kN)	$N_{Rd,sec.}$(kN)	$N/N_{Rd,sec.}$
MFRCH_2			
Experimental	73.10		0.59
SEISMOSOFT	73.26	124.28	0.79
Eurocode	53.26		0.43

4. Conclusions

Based on the Analysis of results obtained from experimental comparing to the theoretical gated from the SEISMOSOFT software and the Eurocode it may conclude.

- A significant difference is observed between the load-bearing capacity calculated according to Eurocode standards and the values obtained from SEISMOSOFT software simulations and experimental methods.
- The numerical calculation was performed by considering only a single column, without accounting for the full scaffold system, which may have led to discrepancies.
- The static scheme of the column, particularly its effective length, plays a crucial role in buckling and stability analysis.
- The numerical model may not fully capture the real boundary conditions and restraints present in the experimental setup, leading to variations in predicted structural behavior.
- A key factor contributing to this difference is the adopted buckling coefficient (effective length factor), which directly impacts the load-bearing capacity of the scaffold system.
- The Design Code, EN 1991-1-1 defines partial safety factors for materials. However, considering the multiple reuses of scaffolding in construction, it is difficult to accurately determine their load-bearing capacity based solely on these parameters. This is because, during transportation, erection, or dismounting, scaffolding elements may undergo deformations that affect their structural performance. For this reason, it is recommended to conduct tests on various types of scaffolds currently in use and compare the obtained results with those of new, unused scaffolds. This approach will help establish a more reliable parameter for the overall safety of scaffold structures.
- Experimental validation is crucial to ensuring accurate safety assessments, particularly for frequently reused scaffolding systems.
- Establishing a revised safety factor based on experimental data will improve reliability and reduce risks in scaffold-supported construction.

5. Declarations

5.1. Author Contributions

Conceptualization, F.G., A.M., D.K., E.S., and Z.G.; methodology, F.G., A.M., and D.K.; software, F.G., A.M., and Z.G.; validation, F.G., A.M., D.K., and Z.G.; formal analysis, F.G., A.M., D.K., and E.S.; investigation, F.G., A.M., D.K., E.S., and Z.G.; resources, F.G., A.M., and D.K.; data curation, F.G., A.M., D.K., and Z.G.; writing—original draft preparation, F.G., A.M., and D.K.; writing—review and editing, F.G., A.M., D.K., E.S., and Z.G.; visualization, F.G. and A.M.; supervision, F.G and E.S.; project administration, F.G., A.M., and D.K.; funding acquisition, F.G., A.M., D.K., and Z.G. All authors have read and agreed to the published version of the manuscript.

5.2. Data Availability Statement

The data presented in this study are available in the article.

5.3. Funding

The authors received no financial support for the research, authorship, and/or publication of this article.

5.4. Conflicts of Interest

The authors declare no conflict of interest.

6. References

[1] EN 1990. (2002). Eurocode-Basis of structural design. European Committee for Standardization, Brussels, Belgium.

[2] EN 1991-1-1. (2002). Eurocode 1: Actions on structures - Part 1-1: General actions - Densities, self-weight, imposed loads for buildings. European Committee for Standardization, Brussels, Belgium.

[3] EN 1993-1-1:2005. (2005). Design of steel structures - Part 1-1: General rules and rules for buildings. European Committee for Standardization, Brussels, Belgium.

[4] BS EN 12811-1:2003 (2003). Temporary Works Equipment - Scaffolds. Performance requirements and general design. British Standards Institution, London, United Kingdom. doi:10.3403/03061625u.

[5] Chu, Q., Liu, H., Xia, S., Dong, J., Lei, M., Tse, T. K. T., Teng, L., Li, C. Y., & Fu, Y. (2022). Numerical and Experimental Study on the Member Performance and Stability Bearing Capacity of Wheel Coupler Formwork Supports. Applied Sciences (Switzerland), 12(20), 10452. doi:10.3390/app122010452.

[6] Lu, Y., Lin, T., & Wu, L. (2025). Experimental study on integrated of steel protective mesh and disk lock scaffold. Journal of Constructional Steel Research, 227, 109321. doi:10.1016/j.jcsr.2024.109321.

[7] Zhang, H., Chandrangsu, T., & Rasmussen, K. J. R. (2010). Probabilistic study of the strength of steel scaffold systems. Structural Safety, 32(6), 393–401. doi:10.1016/j.strusafe.2010.02.005.

[8] Weesner, L. B., & Jones, H. L. (2001). Experimental and analytical capacity of frame scaffolding. Engineering Structures, 23(6), 592–599. doi:10.1016/S0141-0296(00)00087-0.

[9] Huang, H., Peng, Z., Hou, J., Zheng, X., Ding, Y., & Wu, H. (2024). Study on the Ultimate Load-Bearing Capacity of Disc Buckle Tall Formwork Support Considering Uncertain Factors. Buildings, 14(3), 828. doi:10.3390/buildings14030828.

[10] Pieńko, M., & Błazik-Borowa, E. (2020). Experimental studies of ringlock scaffolding joint. Journal of Constructional Steel Research, 173, 106265. doi:10.1016/j.jcsr.2020.106265.

[11] Chandrangsu, T., & Rasmussen, K. J. (2011). Investigation of geometric imperfections and joint stiffness of support scaffold systems. Journal of Constructional Steel Research, 67(4), 576-584. doi:10.1016/j.jcsr.2010.12.004.

[12] Zhang, L., Liu, J., Tang, Q., & Liu, Z. (2023). A numerical study on rotational stiffness characteristics of the disk lock joint. Journal of Constructional Steel Research, 207, 107968. doi:10.1016/j.jcsr.2023.107968.

[13] Do Lee, H., Won, J. H., Jang, N. G., Mha, H. S., Jeong, S. choon, & Kim, S. (2020). Experimental Study on Load Carrying Capacity Enhancement of System Supports Considering Full Installation of Bracing Members. International Journal of Steel Structures, 20(6), 2051–2067. doi:10.1007/s13296-020-00430-5.

[14] Takahashi, H., Ohdo, K., & Takanashi, S. (2011). Experimental study and evaluation method for the buckling strength of scaffold. Procedia Engineering, 14, 297–303. doi:10.1016/j.proeng.2011.07.036.

[15] Kim, H., Lim, J., Lee, J., Kang, Y. J., & Kim, S. (2021). Experimental investigations on ultimate behavior of fabricated mobile scaffolds. Metals, 11(6), 851. doi:10.3390/met11060851.

[16] Peng, J. L., Chen, K. H., Chan, S. L., & Chen, W. T. (2009). Experimental and analytical studies on steel scaffolds under eccentric loads. Journal of Constructional Steel Research, 65(2), 422–435. doi:10.1016/j.jcsr.2008.03.024.

[17] Alqattan, H. F., El Aghoury, I. M., & Ibrahim, S. A. B. (2024). Experimental investigation and analytical modeling of steel falsework systems. Structures, 70, 107623. doi:10.1016/j.istruc.2024.107623.

[18] Mercier, C., Khelil, A., Al Mahmoud, F., Blin-Lacroix, J. L., & Pamies, A. (2021). Experimental investigations of buckling behaviour of steel scaffolds. Structures, 33, 433–450. doi:10.1016/j.istruc.2021.04.045.

[19] Baláž, I., Koleková, Y., Agüero, A., & Balážová, P. (2023). Consistency of Imperfections in Steel Eurocodes. Applied Sciences (Switzerland), 13(1), 554. doi:10.3390/app13010554.

[20] Morel, J. (2005). Calculation of Metallic Structures according to Eurocode 3. Eurocode, Brussels, Belgium. (In French).

[21] ISO 6892-1. (2019). Metallic materials-Tensile testing-Part: Method of test at room temperature. International Organization for Standardization (ISO), Geneva, Switzerland.

[22] EN 10002-1:2001. (2001). Metallic materials—tensile testing: I. Method of test at ambient temperature. European Committee for Standardization, Brussels, Belgium.

[23] Grajçevci, F., Mujaj, A., Kryeziu, D., & Shehu, E. (2024). Experimental and Numerical Analysis of Concrete Columns under Axial Load Based on European Design Norms. Civil Engineering Journal (Iran), 10(2), 419–430. doi:10.28991/CEJ-2024-010-02-05.

[24] Peng, J. L., Wu, C. W., Chan, S. L., & Huang, C. H. (2013). Experimental and numerical studies of practical system scaffolds. Journal of Constructional Steel Research, 91, 64–75. doi:10.1016/j.jcsr.2013.07.028.

[25] Peng, J. L., Wang, P. L., Chan, S. L., & Wu, P. K. (2020). Experimental Study on Load-Bearing Capacities of Frame-Type Scaffolds Used in Precast Construction. International Journal of Steel Structures, 20(2), 400–414. doi:10.1007/s13296-019-00292-6.

[26] Abdel-Jaber, M., Abdel-Jaber, M. S., & Beale, R. G. (2022). An experimental study into the behaviour of tube and fitting scaffold structures under cyclic side and vertical loads. Metals, 12(1), 40. doi:10.3390/met12010040.

[27] Grajçevci, F., Mujaj, A., Kryeziu, D., Rrudhani, G., & Shkodrani, N. (2024). Experimental and Numerical Research on the Behavior of Steel Columns with Circular Hollow Cross Sections. Civil Engineering Journal (Iran), 10(5), 1577–1588. doi:10.28991/CEJ-2024-010-05-014.